Spatial and temporal variability of solar energy

Richard Perez, Mathieu David, Tom Hoff, Sergey Kivalov, Jan Kleissl, Philippe Lauret, & Marc Perez

ABSTRACT
This article summarizes and analyzes recent research by the authors and others to understand, characterize and model solar resource variability. This research shows that understanding solar energy variability requires a definition of the temporal and spatial context for which variability is assessed; and describes a predictable, quantifiable variability-smoothing space-time continuum from a single point to 1000's of km and from seconds to days. Implications for solar penetration on the power grid and variability mitigation strategies are discussed.

INTRODUCTION
Unlike conventional electrical power generation (e.g., fossil or nuclear), solar energy is intermittent. The output of a solar power plant is driven by weather and by the cycle of days and seasons. It varies from zero to full power outside the control of plant operators.

The intermittency, or better termed, variability, of the solar resource has two causes. One is precisely predictable and traceable to the apparent motion of the sun in the sky and the earth's distance from the sun. The other is much less predictable and traceable to the motion of clouds and weather systems.

In order to fully understand the issue and develop intelligent mitigation solutions, both solar geometry-induced variability and cloud-induced variability should be examined in an appropriate spatial and temporal context. Taking an intuitive example for the temporal context, a single location on a given partly cloudy day will experience a high degree of variability due to changes in solar geometry and the passing of clouds. However, solar energy integrated over several days at that same location will exhibit less variability and variability will become insignificant as the temporal integration increases to one year or more (figure 1) – e.g., see Gueymard & Wilcox, (2011). Likewise in the spatial realm, increasing the solar generation footprint from a single location to a resource dispersed over an entire region or a continent will reduce intermittency considerably. Increasing this footprint to the entire planet will eliminate it almost entirely (figure 2).

The focus of this article is placed on understanding, characterizing and modeling the interplay between intermittency and the considered spatial and temporal scales. Implications for the power grid and appropriate intermittency mitigation strategies are discussed.

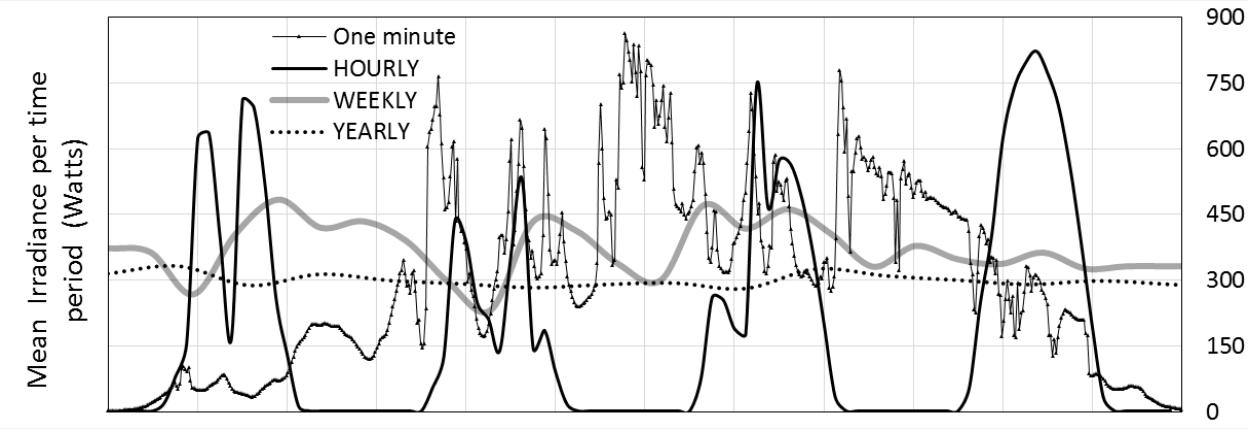

Fig. 1: Comparing the variability of global irradiance time series in a North-American location, as a function of integration time. The figure includes one day's worth of one-minute data, 4 days' worth of hourly data, 26 weeks' worth of weekly data, and 16 years' worth of yearly-integrated data.

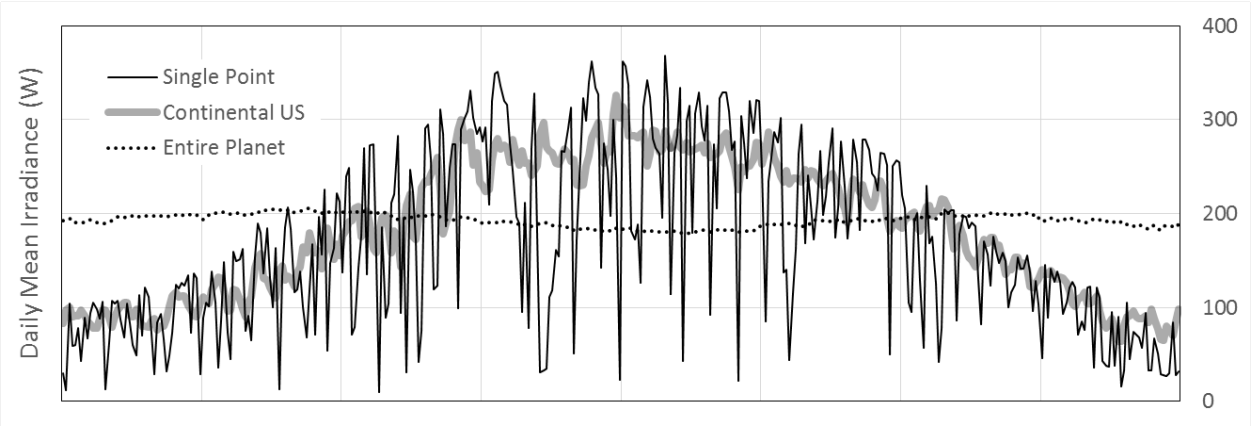

Fig. 2: Comparing the variability of daily global irradiance time series as a function of the considered footprint

QUANTIFYING INTERMITTENCY

How is variability quantified? An appropriate metric must describe: (1) the physical quantity that varies, (2) the variability time scale, and (3) the time span over which variability is assessed.

Physical quantity: The relevant quantity for energy producers and grid operators is the power output, ***p***, of a power plant or an ensemble of power plants at a given point in time. Because ***p*** reflects the underlying variability of impinging irradiance, the fundamental underlying quantities are global irradiance (*GHI*) and direct irradiance (*DNI*). The latter is most relevant for concentrating technologies, while *GHI*'s variability is important for flat plate technologies.

Irradiance variability embeds both predictable solar-geometry, and cloud/weather effects. To focus on the latter, it is helpful to use a normalized quantity that removes solar geometry but conserves cloud-induced variability. The *clearness index, Kt* (ratio of *GHI* to extraterrestrial irradiance) or *the clear sky index, Kt** (ratio of *GHI* to clear sky *GHI*) both meet this criterion although many tend to prefer *Kt**

because it more effectively removes solar geometry effects at lower solar elevations (e.g., see Perez et al., 1990) and has a more intuitive range.

Time scale: The above intuitive temporal example suggests that the time period, or its inverse the frequency, of the selected physical quantity's time series is an essential factor. Having defined the physical quantity, e.g., Kt^*, its changes $\Delta Kt^*_{\Delta t}$ over a given period Δt are often referred to as ramp rate. The time interval can range from a few seconds to hours and more depending on the concern of the user.

Time span: A proper measure of variability should include ramp events over a statistically significant *time span*. This time span should be a large multiple of Δt.

Nominal variability metric: Nominal variability refers to the variability of the dimensionless clear sky index. The maximum or mean $\Delta Kt^*_{\Delta t}$ ramp rate over a given time span has been proposed as such a measure (e.g., Hoff & perez, 2010) However most authors prefer using the ramp rate's variance, or its square root, the ramp rate standard deviation, over a given time span as the metric for variability. We retain this definition of *nominal variability*.

$$\textit{Nominal Variability} = \sigma(\Delta Kt^*_{\Delta t}) = \sqrt{Var[\Delta Kt^*_{\Delta t}]} \quad (1)$$

Historically, there has been other approaches to quantify variability. In earlier work, Skartveit & Olseth (1992) have used of the standard deviation of *Kt,* σKt, rather than $\sigma \Delta Kt$ or $\sigma \Delta Kt^*$ as a measure of variability. However the latter should be a more appropriate metric because σKt can be driven by one single ramp event -- consider for instance the case of perfectly clear conditions (i.e., no variability) followed by a one-time change to uniform, heavily overcast conditions without variability; in this case σKt would be the same as if conditions were highly variable and changing from clear to cloudy at every time period; on the other hand $\sigma \Delta Kt^*$ would capture the difference between the two situations with a low value in the first case and a high value in the second.

Power output (absolute) variability: Eq. 1 describes a nominal dimensionless metric. When dealing with power generation it is also useful to quantify variability in absolute terms. This is expressed by Eq. 2.

$$\textit{Power Variability} = \sigma(\Delta \boldsymbol{p}_{\Delta t}) = \sqrt{Var[\Delta \boldsymbol{p}_{\Delta t}]} \quad (2)$$

VARIABILITY MITIGATION – SPATIAL AND TEMPORAL EFFECTS

When considering a fleet of multiple solar electric installations the power variability of N plants is given by (Hoff & Perez, 2012, Perez & Hoff, 2013):

$$Fleet\ Power\ Variability = \sigma(\textstyle\sum_{n=1}^{N} \Delta \boldsymbol{p}^{\boldsymbol{n}}_{\Delta t}) = \sqrt{Var[\sum_{n=1}^{N} \Delta \boldsymbol{p}^{\boldsymbol{n}}_{\Delta t}]} \quad (3)$$

Where p^n represents the power output time series of the n[th] plant in the fleet.

In the special case where all the plants in the fleet are identical, exhibit the same variability$\sigma(\Delta \boldsymbol{p}_{\Delta t})$, and their power output time series are *uncorrelated,* Eq. 3 simplifies to:

$$Fleet\ Power\ Variability = \sqrt{N\ Var[\Delta \boldsymbol{p}_{\Delta t}]} = \sqrt{N}\sigma(\Delta \boldsymbol{p}_{\Delta t}) \qquad (4)$$

In this special case, the *relative variability* – defined as the ratio of absolute variability to installed capacity – is given by:

$$Fleet\ Relative\ Variability = \frac{\sqrt{N}\sigma(\Delta \boldsymbol{p}_{\Delta t})}{NP_{installed}} \qquad (5)$$

Where $P_{installed}$ is the installed capacity of each plant. Therefore the relative variability of a fleet of identical power plants with uncorrelated power outputs, but experiencing the same level of individual variability equals each individual plant's relative variability divided by the square root of the number of plants.

$$Fleet\ Relative\ Variability = (Single\ Plant\ Relative\ Variability)/\sqrt{N} \qquad (7)$$

More generally, Eq. 7 is applicable to the nominal variability of a fleet of N locations experiencing identical, but uncorrelated *Kt** time series.

$$\sigma_{\Delta t}^{Fleet} = \frac{\sigma_{\Delta t}^{1}}{\sqrt{N}} \qquad (7)$$

Where $\sigma_{\Delta t}^{Fleet}$ is the fleet's nominal variability and $\sigma_{\Delta t}^{1}$ is a single location's nominal variability.

This relative variability reduction underlies the well-known *spatial smoothing effect* noted by many authors – e.g., Marcos et al., (2013), Murata et al., (2009), Woyte et al., (2007), Wiemken et al., (2001), Vignola, 2001).

Nearby locations are highly correlated, experiencing the same ramp rates at the same time and varying in sync; in this case the fleet exhibits nearly the same relative variability as the individual systems. Distant locations' time series are uncorrelated; hence the fleet's relative variability is reduced by $\sqrt{N}$. Therefore the key factor to capture is correlation. A considerable amount of work has been devoted to this issue in recent years – e.g., Becker et al., (2014), Bing et al., (2011), Badosa et al., (2013), Frank et al., (2011), Halász & Malachi, (2014), Hoff & Norris (2010), Hoff & Perez, (2012b), Huang et al., (2014), Jamaly et al., (2012), Kankiewicz et al., (2011),Kuszamaul et al., (2010), Lave et al., (2013), Lave & Kleissl, (2013), Lorenz et al., (2011), Mazumbdar et al., (2013), Norris & Hoff, (2011) Perez et al., (2011a, 2011b,

2012), Rowlands et al., (2014), Sengupta (2011), Stein et al., (2011), Vindel & Polo (2014) -- leading to the assertion that the correlation of $\Delta Kt^*_{\Delta t}$ time series between two locations is a predictable function of three factors:

- The distance, d, between the two locations,
- The time scale, Δt,
- The speed, *V*, of the variability-inducing clouds/weather systems[1].

The central influence of time, speed and distance had been identified by Hoff & Perez (2010) who postulated that a dimensionless *dispersion factor*, *D,* captures the variability relationship between a single point and a dispersed PV fleet. The dispersion factor is given in Eq. 8 for a homogenous fleet of systems, where L represents the linear dimension of the fleet in the wind direction.

$$D = \frac{L}{V\Delta t} \quad (8)$$

They identified three possible fleet configurations (figure 3):

(1) A *crowded configuration* where the number of systems, N, exceeds the dispersion factor. In this case the relative variability of the fleet equals the single point's relative variability divided by D.
(2) An *optimum configuration* where D equals N and where the fleet's variability equals the single point's variability divided by N.
(3) A *dispersed configuration* where D is larger than N and where the fleet's variability asymptotically tends towards the single point's variability divided by $\sqrt{N}$ as D/N increases.

[1] *This velocity is a priori defined as the vector in the direction of the two considered locations. However, as will be discussed below, empirical evidence shows that a mean, local -- directionless -- velocity, can be an adequate input for assessing regional station pair correlations.*

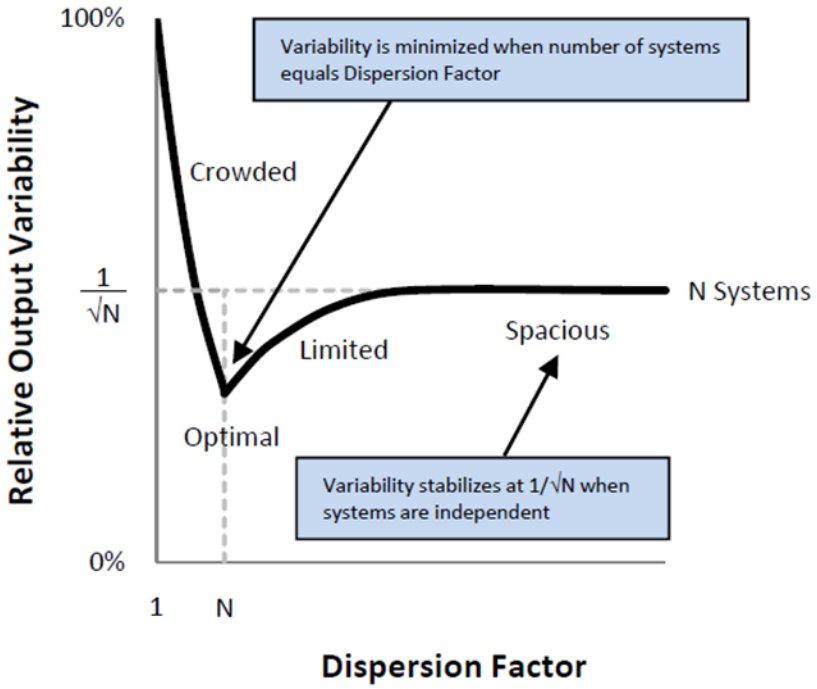

Fig. 3: Relative output variability as a function of the Dispersion Factor for a fleet of N identical PV systems experiencing the same individual variability

The dispersion factor model reflects the underlying correlation (or anti-correlation) existing between any two points within the fleet. Considering a single pair of stations experiencing the same nominal variability $\sigma_{\Delta t}^{1}$, Eq. 7 may be generalized when the two locations are partially correlated, leading to:

$$\sigma_{\Delta t}^{pair} = \frac{\sqrt{\rho+1}}{\sqrt{2}}\,\sigma_{\Delta t}^{1} \qquad (8)$$

Where $\sigma_{\Delta t}^{pair}$ is the nominal variability of the pair and $\boldsymbol{\rho}$ is the correlation between each time series.

The dependence of $\boldsymbol{\rho}$ upon Δt, d, and V has been inferred from a growing base of empirical evidence.

Mills & Wiser (2010) analyzed 20 second data from the 32-station ARM network (Stokes & Schwartz, 1994). They observed the exponential decay of station pair correlation as a function of station distance and noted that the rate of decay was a continuous function of the considered time scale. Hoff & Perez, (2012) used 10 km hourly satellite-derived irradiances over the continental US. They observed a similar asymptotic decay with distance and a predictable dependence of this decay upon Δt for time intervals of 1, 2 and 3 hours. They also noted that the rate of decrease of correlation with distance was different for different US regions and attributed these differences to prevailing regional cloud speeds. Hoff et al. (ref) analyzed high frequency data (seconds) from a 25-station modular network and confirmed that asymptotic decay with distance was a strong function of Δt depending on cloud speed that they had

acquired independently from satellite-derived cloud motion vectors. They proposed the following relationship linking distance, time interval and cloud speed.

$$\rho = \frac{1}{1+\frac{d}{(\Delta t)(V)}} \qquad (9)$$

Perez et al. analyzed high-resolution high-frequency satellite-derived irradiances (1km, 1minute) in climatically distinct regions of North America and Hawaii to investigate site-pair correlation decay as a function of distance (0-200km) time scale (1 minute to hourly) and mean monthly regional cloud speed (figure 4) independently derived from satellite cloud motion vectors. They proposed an alternate formulation for ρ given in Eq. 10:

$$\rho = e^{\frac{d\ln(0.2)}{1.5\,(\Delta t)(V)}} \qquad (10)$$

Lave & Kleissl (2010) and Lave et al. (2011) analyzed high-resolution distributed irradiance measurements with a variety of statistical tools such as spectra, coherence spectra, wavelet, correlations, probability density functions, and spatial and temporal averaging with the objective of developing a model for simulating the power output of large power plants from single point measurements. The wavelet variability model (WVM) was then proposed in Lave et al. (2013a) and it uses wavelet decomposition of the irradiance signal into different time scales (duration of shading from clouds or clouds systems, (figure 5) that were proven to be associated with different amounts of variability reduction. The associated preliminary spatio-temporal correlation function dictates the amount of variability reduction and uses a parameter *A* that scales the correlation function and that had to be determined from a sensor network collecting high frequency irradiance data.

$$\rho = exp\left(-\frac{d}{A\,\bar{t}}\right) \qquad (11)$$

Through a virtual cloud model Lave et al. (2013b) inferred that the parameter A in Eq. 11 could be approximated to ½ *V* for station pairs in the direction of the cloud speed.

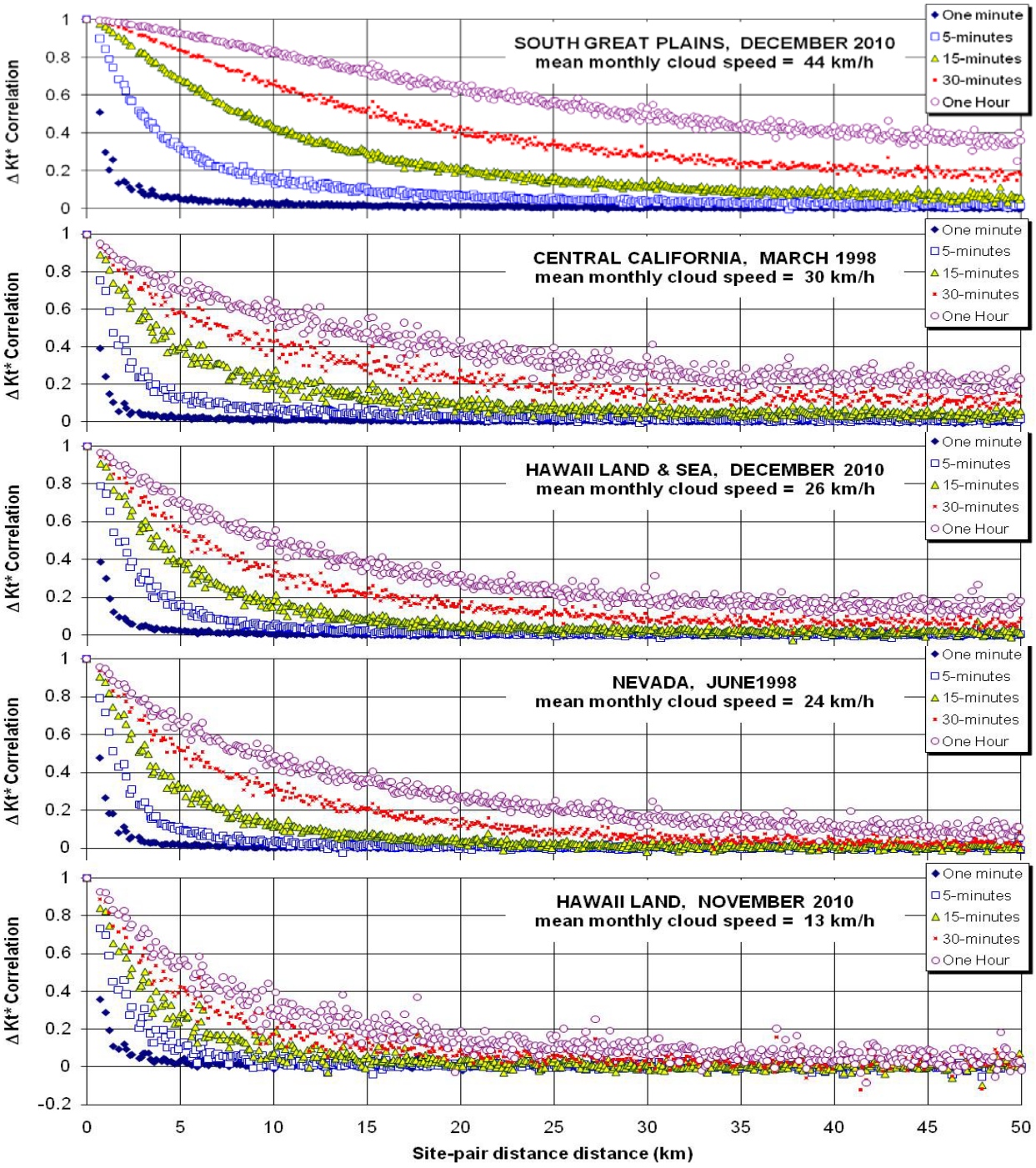

Fig. 4: Site-pair correlation as a function of time period and distance for sample regions in North America and Hawaii. Mean monthly cloud speed was estimated from satellite-derived cloud motion vectors computed for each data point.

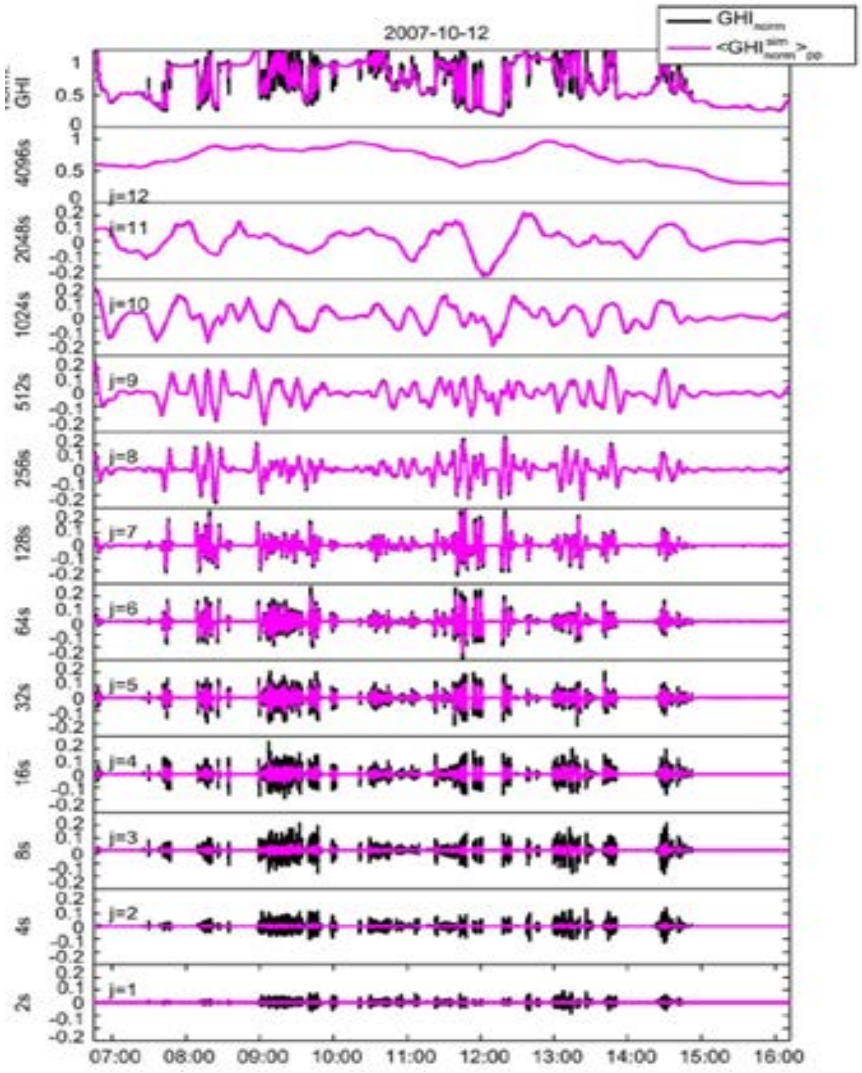

Fig. 5: (Top plot): Clear-sky index time series, and (bottom 12 plots) wavelet modes for Ota City on October 12, 2007. Clear-sky index measured (GHI, black) and simulated spatially averaged across the power plant (GHI, magenta). The spatial smoothing is especially evident for the short time scales, but it essentially disappears at a time scale of 2 to 5 minutes.

Figure 6 illustrates and contrasts the formulations in Eq. 9, 10 and 11 for an example with a time scale of one minute and a cloud speed of 20 km/hour. Note that the difference between Eq. 10 and 11 may be traceable to the fact that V represents a monthly prevailing cloud speed in the first case and a time-coincident cloud speed in the second, further noting that Eq. 10 was derived empirically without consideration whether pairs where located along or across wind direction.

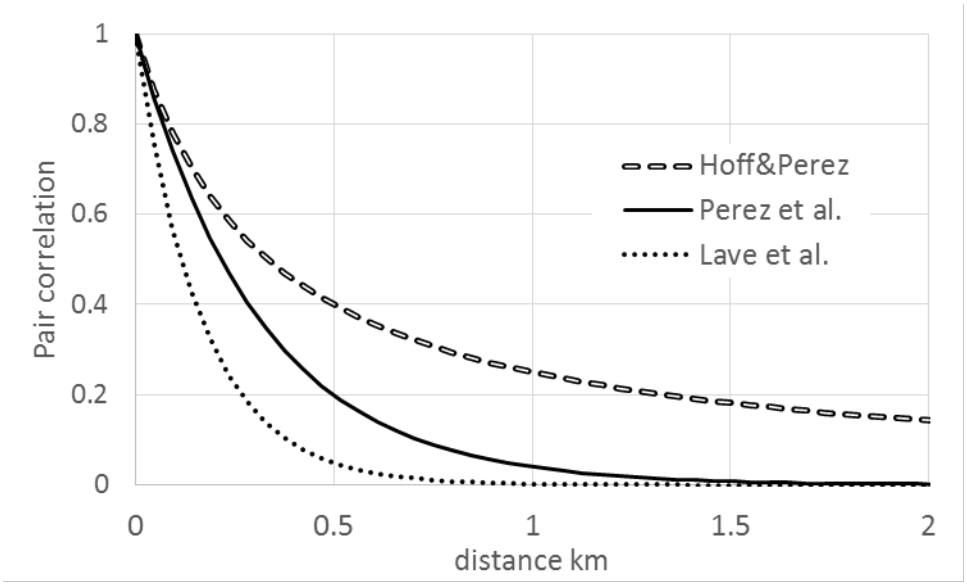

Fig. 6: Comparing correlation decay with distance as formulated in Eq. 9, 10 and 11 for one-minute data and a cloud speed of 20 km/h.

Formulations such as equation 9 or 11 that define cloud speed in the direction of a station pair, do not explain the variability and correlation reduction with distance that is nevertheless observed when speed is zero – i.e., in cross wind directions – e.g., see Hinkelmann et al., (2011), Lonji et al., (2013) -- Solar Energy 97 58-66 2013]. As an attempt to describe correlation anisotropy with respect to cloud speed, Arias-Castro et al. (2013) applied a kinematic-stochastic model based upon given cloud cover fraction λ_n, cloud size r, stream-wise and cross-stream distance, cloud speed, and time difference. Through dimensional analysis, the correlation functions were expressed through just 4 independent variables: cloud cover fraction, the along-wind and cross-wind distance normalized by cloud diameter (D_{along}, D_{cross}), and the distance of cloud motion within the ramp interval Δt relative to the cloud diameter (D_{cloud}) resulting in Eq. 12.

$$\rho = \frac{2\mathrm{e}^{-\lambda_n\left[2-A_n\left(\sqrt{{D_{along}}^2+{D_{cross}}^2}\right)\right]} - \mathrm{e}^{-\lambda_n\left[2-A_n\left(\sqrt{(D_{along}-D_{cloud})^2+{D_{cross}}^2}\right)\right]} - \mathrm{e}^{-\lambda_n\left[2-A_n\left(\sqrt{(D_{along}+D_{cloud})^2+{D_{cross}}^2}\right)\right]}}{2[\mathrm{e}^{-\lambda_n} - \mathrm{e}^{-\lambda_n[2-A_n(D_{cloud})]}]} \quad (12)$$

Further, the three key factors governing the correlation decay -- time scale, cloud speed and distance -- are not entirely independent variables. This was noted by David et al. (2014) when they analyzed station pair correlations from an irradiance measurement network in the Island of la reunion. Whereas exponential formulation in Eq. 10 and 11 would imply that, for a given cloud speed, a linear relationship should exist between the distance at a given correlation level and time scale, with the slope depending on cloud speed, (Perez et al., 2011a), they observed that the time scale vs. distance slope tended to diminish as a distance increased (figure 7). This may be explained by the observation that the underlying driver of variability (cloud speed) evolves as a function of the considered spatial and temporal scales. For the smallest scales the drivers are cloud substructures. As the spatial scale increases, the drivers become

entire cloud fields, and then entire weather systems, hence because the speed of these drivers is known to decrease with scale, the observed relationships are non-linear.

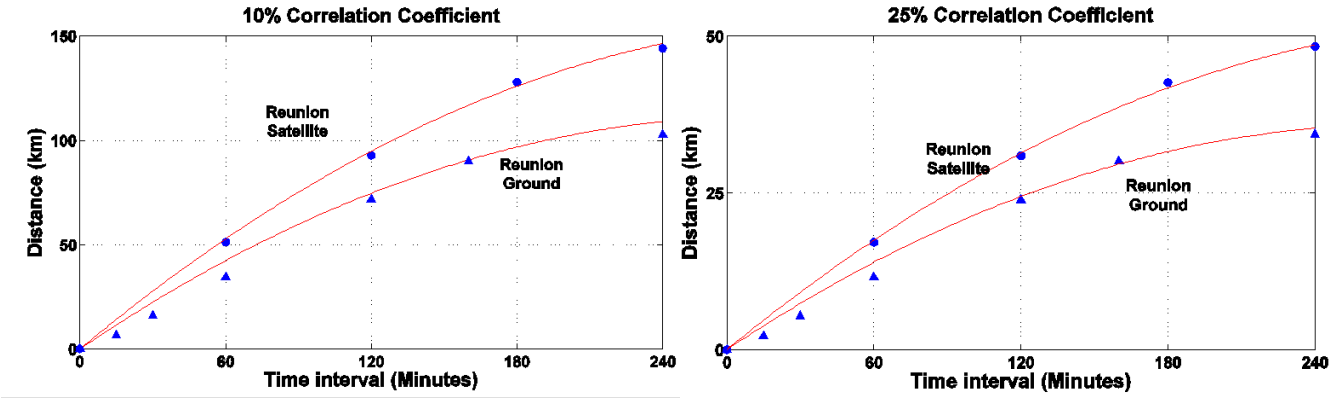

Fig. 7: Mean distance to reach a 10% (left) and a 25% (right) correlation threshold as a function of the time interval of observations in La Reunion (ground and satellite)

The cloud speed dependence upon time scale becomes fully apparent when considering very large spatio-temporal scales as in Perez & Fthenakis (2012, 2015) who analyzed millions of possible pair correlations from the NASA SSE data set (NASA, 2012) for the entire planet. Figure 8 compares the observed exponential correlation decay for ΔT of one and seven days respectively. It is remarkable that these results are fully consistent with lower spatio-temporal scales such as shown in figure 4, plausibly representing an expression of the underlying self-similar (fractal) nature of clouds and cloud systems at all scales (Lovejoy, 1982). As for smaller scales, decorrelation distances are a function of prevailing cloud speed. Comparing East-West pairs and North-South pairs in Figure 9 indicates that decorrelation distances are considerably shorter for the latter – a manifestation of the fact that weather systems tend to move in East-West directions. Finally, as noted for la Reunion it is also apparent that the cloud system velocity underlying variability decreases with time scale. For instance, cloud system speeds inferred from figure 9 using equation 10 would indicate that the speed of the East-West weather system motion driver for daily ΔT is of the order of 20 km/h. For ΔT of seven days the prevailing weather system's speed is of the order of 8 km/h.

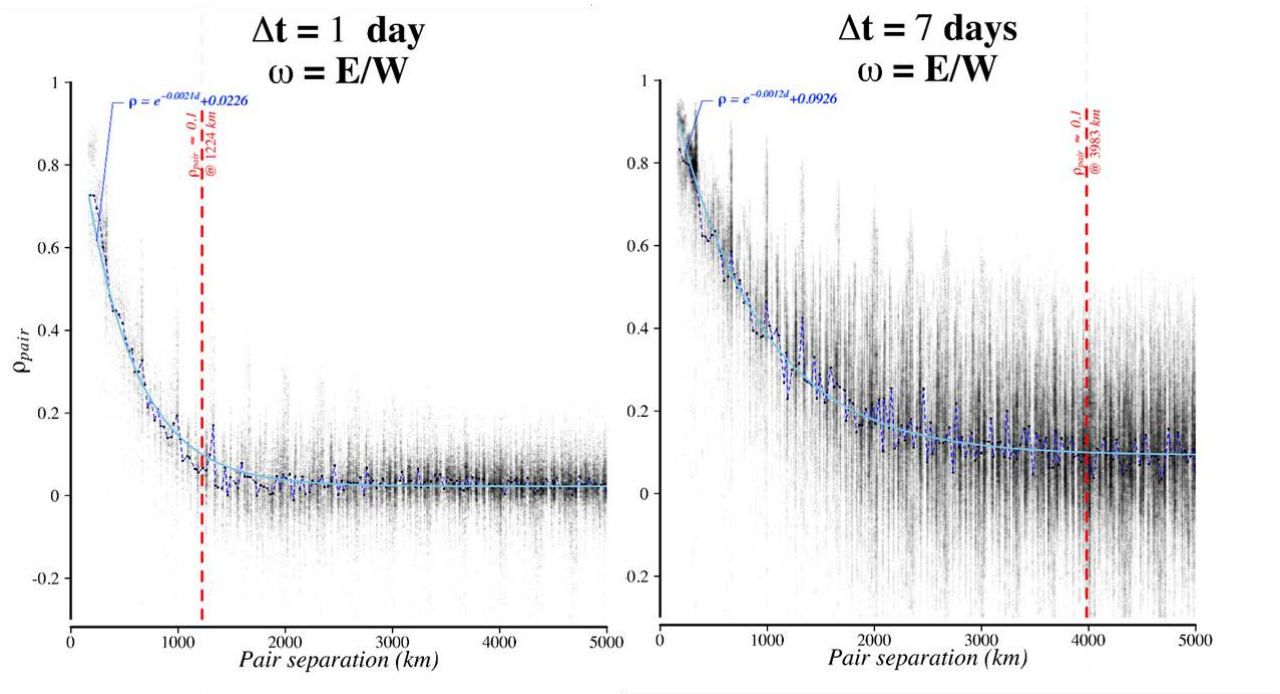

Fig. 8: Site-pair correlation as a function distance for daily and weekly time periods. Station pairs are selected to have a predominantly East-West orientation.

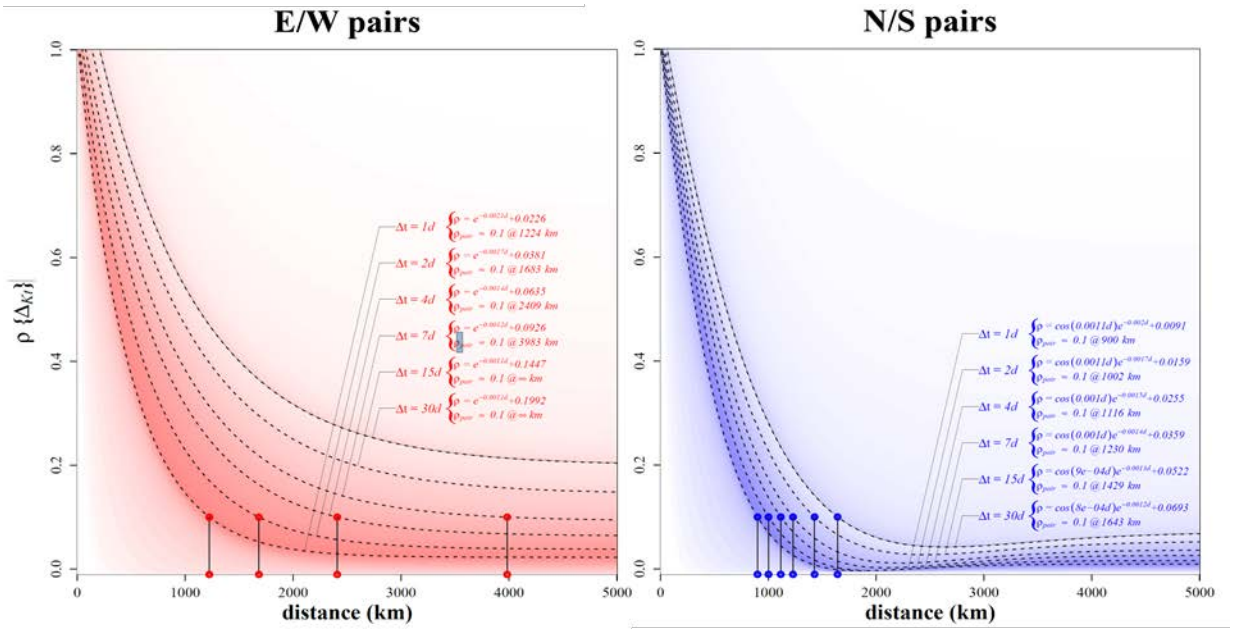

Fig. 9: Impact of prevailing cloud speed on correlation decay for time periods ranging from one to thirty days – contrasting East-West pairs (prevailing direction of weather systems) and North-South pairs

APPLICATION MODELS AND TOOLS:

Understanding the fundamentals of solar resource variability's spatio-temporal characteristics has led to the development of tools and methodologies to address operational questions, in particular to address the question of how to predict the variability and output ramp-rates of spatially extended or distributed solar power plants from a limited number of input data, e.g., a single pyranometer.

An approach developed by Lave et al., applies the wavelet analysis to decompose the irradiance signal into different time scales (see fig. 5 above) to simulate a power plant's output given (1) a spatio-temporal correlation function (e.g., from eq. 11), (2) measurements from a single irradiance point sensor, (3) knowledge of the power plant footprint and PV density (Watts of installed capacity per m^2), (4) a time and location-dependent scaling parameter (parameter A in Eq. 11). The WVM uses these inputs to estimate the variability ratio over the area of the plant. The simulated power plant may have any density of PV coverage: it may be distributed generation with low PV density (i.e., a neighborhood with rooftop PV), centrally located PV as in a utility-scale power plant with high PV density, or any combination of both.

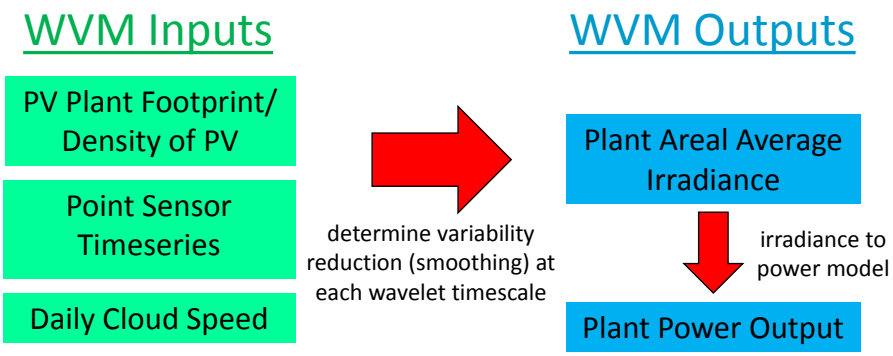

Fig. 10: Wavelet variability model (WVM) for modeling reduction in PV power output variability through geographic smoothing.

Another operational approach proposed by Hoff & Perez is based upon expressing Eq. 3 as the sum of the covariance of all possible plant pair combinations in a PV fleet.

$$\sigma_{\Delta t}^{fleet} = \sqrt{Var[\sum_{n=1}^{N} \Delta \boldsymbol{P}_{\Delta t}^{\boldsymbol{n}}]} = \sqrt{\sum_{i=1}^{N}\sum_{j=1}^{N} COV\left(\Delta \boldsymbol{P}_{\Delta t}^{\boldsymbol{i}}, \Delta \boldsymbol{P}_{\Delta t}^{\boldsymbol{j}}\right)} \qquad (12)$$

The covariance between any two plants equals the standard deviations of each of the locations times the correlation coefficient between the two locations (i.e. $COV\left(\Delta \boldsymbol{P}^{\boldsymbol{i}}_{\Delta \boldsymbol{t}}, \Delta \boldsymbol{P}^{\boldsymbol{j}}_{\Delta \boldsymbol{t}}\right) = \sigma^{i}_{\Delta t}\sigma^{j}_{\Delta t}\rho^{i,j}_{\Delta t}$). Therefore the standard deviation of the changes in fleet output can be defined entirely by the standard deviation of the change in plant output at each location and the correlation between the locations (obtained e.g., from Eq. 10). This method can be applied by deriving nominal variability from one, or a small subset of instrumented stations and assuming that sampled variability is representative of nearby locations.

Kato et al. (2011) proposed a comparable approach to determine fluctuation of high penetration photovoltaic power generation system dispersed over a large area known as the representative blocks method. PV is distributed over a number of subgroups each consisting of N blocks with a given installed capacity and a given variability. The size of each block is set so as block to block correlation is negligible and a form of Eq. 5, accounting for different system sizes, may be applied to aggregate blocks and determined the variability of the ensemble.

The methodologies developed to understand variability have also led to the development of new instrumentation and modeling capabilities for generating high frequency data over extended areas. The sky imager functionality has been greatly enhanced -- Urquhart et al. (2014), to produce high frequency (seconds) locally gridded irradiance data (~10 km radius) and cloud speed can be measured as input to variability models (Fung et al., (2013) Bosch et al., (2013a, 2013b))--. Satellite-to-irradiance models were also enhanced to produce high resolution (1 km) data with a time scale approaching 1-minute (Perez et al., 2011a). In addition to producing the experimental data that led to a better understanding of variability, these new capabilities, in particular the satellite capability, have also led to a direct massive approach of PV fleet simulation to directly evaluate and manage variability issues for time scales in excess of a few minutes and spatial scales of a few kilometer, by directly simulating any dispersed PV fleets from satellite-derived irradiance time series (Clean Power Research, 2012.)

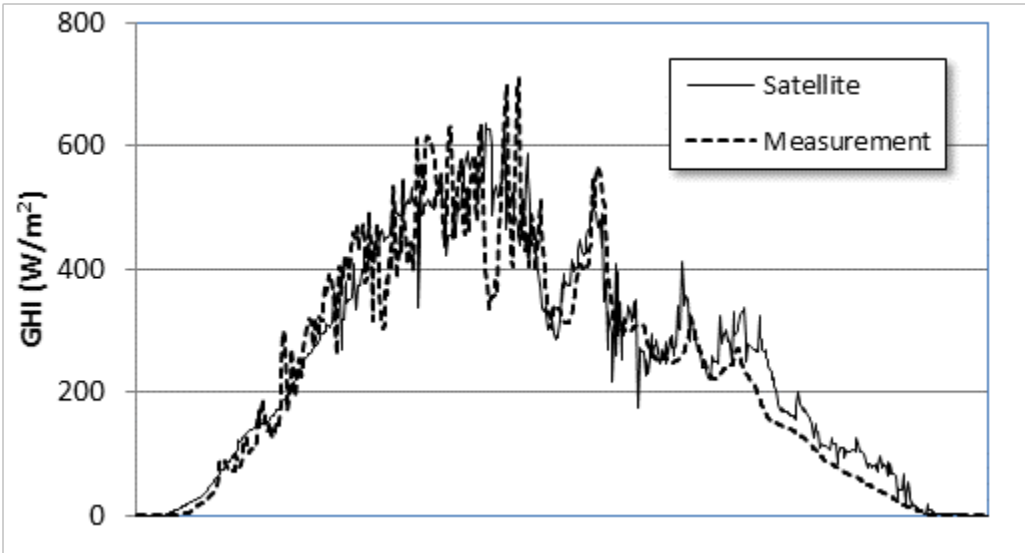

Fig. 11: Comparing one-minute satellite-derived and measured global irradiance

SOLAR VARIABILITY: IMPLICATIONS FOR POWER GRID MANAGEMENT

Observations and models describe a space-time continuum underlying the smoothing effect solar resource variability: shortest-term variability matters for the smallest spatial scales while the minimum relevant time scale gradually increases with the size of the considered footprint. This is illustrated in Figure 12 where the absolute power variability of a nominal 1kW PV power plant (from eq. 2) is plotted as a function of the resource's footprint from a single point up to 200X200 km. This particular example is set in a tropical locations. However trends observed in different climates are quite comparable (Perez et al., 2013b).

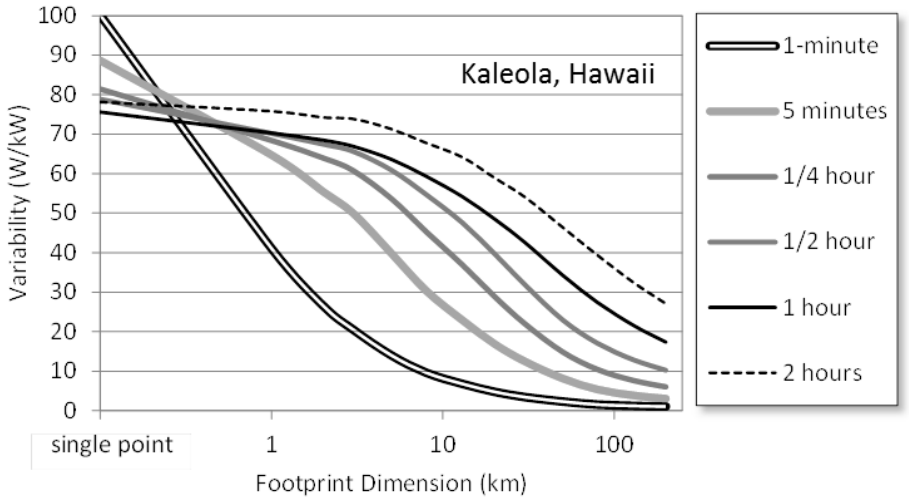

Fig. 12: Nominal variability of a 1 kW power plant as a function of its footprint

The solar generation footprint and time scale should therefore be the primary concerns of grid operators as they pose different load management challenges and imply different solutions: for single distribution systems and large centralized plants, one-minute fluctuations are relevant as they may create voltage control issues. For grid balancing areas including both fleets of large and small distributed systems, variability effects below 30 minutes should be of no concern, while hourly and above time scales remain relevant. .

Likewise variability mitigation solutions should reflect the solar resource time-space context.

- Up to 10s of meters – small and medium PV installations -- ramp rates of the order of seconds are relevant – in particular over-irradiance issues, where ramps can exceed power ratings by up to 50% (Ole-Morten, 2014, Yordanov et al., 2012) and can create voltage control issues at interconnection points. These are generally passively mitigated by the installations' hardware that curtails excess spikes. For very large systems, buffering via capacitors may be warranted.

- From hundreds of meters to a few km -- distribution feeders and large PV plants -- minute ramps are relevant, with impact on distribution system voltage, or transmission system voltage for large centralized power plants. In the latter case active output buffering via capacitor or battery storage could be considered – some utilities impose maximum allowable one-minute ramp rate requirements (PEA, 2013). However these should only be warranted for very large plants or very dense PV fleets where solar production is of the order of the base demand energy flow on the local power grid. For most distributed systems, as long as penetration remains reasonable, experience shows that the ramping noise induced by PV systems on distribution grids is less than the background demand-side ramp noise that utilities have been accustomed to handle for a long time (Holger et al., 2014, 2014a). For very large dispersed penetration -- exceeding local demand -- grid management would be similar to a centralized plant case and would require buffering
- From 5 to 20 km – substations, cities -- 1 minute variability vanishes while 10 minute and longer ramps remain. Depending on penetration, local regulation via storage may be needed.
- For ~ 50 km – large cities and dense transmission networks -- 15-30 minutes fluctuations and above are still a concern. Solutions include contingency stand-by generation, storage or load management in order to react to ramps and insure balance between supply and demand -- note that these solutions need not be collocated with PV installations.
- For 100's km – regional transmission organization's balancing areas – fluctuations of less than one hour should not be of concern. Variability mitigation at these scales can be effectively handled by an optimized basket of active generation, storage, load management, PV output curtailment, and increased interconnection bandwidth (Perez, 2015).

For all temporal and spatial scales where active variability mitigation would be needed, it has been shown that solar forecasting could substantially reduce mitigation measures and operational cost (Perez et al., 2013b). For small centralized scales, minutes-ahead forecasts could be obtained from sky imaging sensors (Yang et al., 2014), while for a few km and more, satellite-derived (1-2 hours ahead) and numerical weather prediction forecasts (5+ hours ahead) would be warranted (Perez et al., 2014).

CONCLUSIONS

The understanding of solar energy variability requires a specification of the temporal and spatial context for which variability is assessed. A large body of work has been produced in recent years which has led to the understanding of a predictable, quantifiable variability-smoothing space-time continuum from a single point to 1000's of km and from seconds to days. The shortest relevant time scale for which variability should be assessed is a direct function of the considered solar generation footprint, and, to a lesser extent, the speed of the clouds/weather systems inducing variability.

The impact of solar variability on power grids can only be assessed, and if needed mitigated, under this space-time contextual light. For instance whereas the mitigating of one-minute ramps is warranted for

large centralized plants, it would be both inefficient and useless for a fleet of small and medium systems distributed over a utility service area, where mitigation occurs naturally.

ACKNOWLEDGEMENT

- Many Thanks to Juan Bosch of Clean Power Research for constructive comments.
- Part of the work presented in this paper was undertaken under the auspices of IEA-SHCP Task 46 – David Renné, Operating Agent.

REFERENCES

Arias-Castro, E., J Kleissl, M Lave, J Schweinsberg, R Williams, (2013): A Poisson model for anisotropic solar ramp rate correlations, Solar Energy, 101:192-202.

Badosa, J., Haeffelin, M., Chepfer, H. (2013): Scales of Spatial and Temporal Variation of Solar Irradiance on Reunion Tropical Island. Solar Energy 88:42-56

Becker, S. et al. (2014): Features of a fully renewable US electricity system: Optimized mixes of wind and solar PV and transmission grid extensions. Energy 72: 443-458

Bing J., P. Krishnani, O. Bartholomy, T. Hoff and R. Perez. (2012): Solar Monitoring, Forecasting, and Variability Assessment at SMUD. Proc. World Renewable Energy Forum, Denver, CO

Bosch JL, Kleissl J, (2013a): Cloud motion vectors from a network of ground sensors in a solar power plant, Solar Energy, 95:13-20.

Bosch JL, Y Zheng, J Kleissl, (2013b): Deriving cloud velocity from an array of solar radiation measurements, *Solar Energy*, 87: 196-203

Clean Power Research (2012): "Behind-the-Meter Intelligence for Distributed PV Grid Integration" Whitepaper available online at http://www.cleanpower.com/wp-content/uploads/SA-FleetView-Whitepaper-v060812.pdf

David, M., F. Andriamasomanana and O. Liandrat, (2014): Spatial and Temporal Variability of PV Output in an Insular Grid: Case of Reunion Island. Energy Procedia, 57, 1275-1282.

Frank, J., J. Freedman, M. Brower and M. Schnitzer, (2011): Development of High Frequency Solar Data, Proc. Solar 2011, American Solar Energy Society Conf., Raleigh, NC

Fung, V., JL Bosch, S Roberts, J Kleissl, (2013): .: Cloud shadow speed sensor, Atmos. Meas. Tech., 7, 1693-1700, doi:10.5194/amt-7-1693-2014, 2014.

Halász, G., Malachi, Y. (2014): Solar Energy from Negev Desert, Israel: Assessment of Power Fluctuations for Future PV Fleet. Energy for Sustainable Development, 21:20-29

Hinkelmann L., R. George and M. Sengupta, (2011): Differences between Along-Wind and Cross-Wind Solar Variability. Proc. Solar 2011, American Solar Energy Society Conf., Raleigh, NC

Holger R., M. Schroedter-Homscheidt, F. Meier and G. Heilscher, (2014): Application of meteorological data for state estimation of an electrical low voltage grid with a high amount of photovoltaic systems 14th EMS Annual Meeting & 10th European Conference on Applied Climatology (ECAC), Prague.

Holger R., M. Schroedter-Homscheidt, H. G. Beyer, F. Meier and G. Heilscher, (2014a): Wolkenindikatoren für die Sammelschienenspannung von Niederspannungsverteilnetztransformatoren, 29. Symposium Photovoltaische Solarenergie. 12. bis 14. März 2014,Kloster Banz, Bad Staffelstein;

Hoff, T.E., Norris, B. (2010): Mobile High-Density Irradiance Sensor Network: Cordelia Junction Results

Hoff, T. E., and Perez, R. (2010): "Quantifying PV power Output Variability." Solar Energy 84 (2010) 1782–1793.

Hoff T., & R. Perez (2012): Modeling PV Fleet Output Variability, Solar Energy 86, 8, 2177-2189

Hoff, T.E., and R. Perez, (2012b): Predicting Short-Term Variability of High-Penetration PV. Proc. World Renewable Energy Forum, Denver, CO.

Huang, J., Troccoli, A., Coppin, P. 2014. An analytical comparison of four approaches to modelling the daily variability of solar irradiance using meteorological records. Renewable Energy 72:195-202

Jamaly, S., Bosch, J., Kleissl, J. (2012): "Aggregate Ramp Rates of Distributed Photovoltaic Systems in San Diego County." IEEE Transactions on Sustainable Energy, in press

Kankiewicz A., M. Sengupta and J. Li, (2011): Cloud Meteorology and Utility Scale variability. Proc. Solar 2011, American Solar Energy Society Conf., Raleigh, NC

Kato, T., T. Inoue and Y. Suzuki, (2011): Estimation of Total Power Output Fluctuation of High Penetration Photovoltaic Power Generation System. Proc. IEEE Power and Energy Society General Meeting, Detroit, Michigan, USA, 2011

Kuszamaul, S., Ellis, A., Stein, J., Johnson, L. (2010): "Lanai High-Density Irradiance Sensor Network for Characterizing Solar Resource Variability of MW-Scale PV System." 35th Photovoltaic Specialists Conference, Honolulu, HI. June 20-25, 2010

Lave M, Kleissl J, 'Solar Intermittency of Four Sites across the State of Colorado', Renewable Energy, 35:2867-2873, 2010.

Lave, M., J. Kleissl, Arias-Castro, E., High-frequency fluctuations in clear-sky index, *Solar Energy*, doi:10.1016/j.solener.2011.06.031, 2011.

Lave M, J Kleissl, J Stein, (2013a): A Wavelet-based Variability Model (WVM) for Solar PV Powerplants, IEEE Transactions on Sustainable Energy, 99, 2012, 10.1109/TSTE.2012.2205716.

Lave, M, J Kleissl, (2013b) Cloud Speed Impact on Solar Variability Scaling - Application to the Wavelet Variability Model, Solar Energy, 91:11-21, 10.1016/j.solener.2013.01.023., 2013.

Lonij, V., A. Brooks, A. Cronin, M. Leuthold, K. Koch, (2013): Intra-hour forecasts of solar power production using measurements from a network of irradiance sensors Solar Energy 97, 58-66.

Lorenz E., T. Scheidsteger, J. Hurka, D. Heinemann and C. Kurz, (2011): Regional PV power prediction for improved grid integration. Progress in Photovoltaics, 19, 7, 757-771.

Lovejoy, S., (1982): Area-Perimeter Relation for Rain and Cloud Areas. Science, New Series, Vol. 216, No. 4542, 185-187

Marcos J., L. Morroyo, E. Lorenzo and M. Garcia, (2012): Smoothing of PV power fluctuations by geographical dispersion. Prog. Photovolt: Res. Appl. 2012; 20:226–237

Mazumdar, B.M., Saquib, M., Das, A.K. (2013): An Empirical Model for Ramp Analysis of Utility-Scale Solar PV Power. Solar Energy 107:44-49

Ole-Morten, M., G. Yordanov and I. Ranaweera, (2014): Short-Term Intermittency of Solar Irradiance in Southern Norway. Proceedings 29th European Photovoltaic Solar Energy Conference and Exhibition. WIP Renewable Energies 2014 ISBN 3-936338-34-5. s. 2635-2638

Murata, A., H. Yamaguchi, and K. Otani (2009): A Method of Estimating the Output Fluctuation of Many Photovoltaic Power Generation Systems Dispersed in a Wide Area, Electrical Engineering in Japan, Volume 166, No. 4, pp. 9-19

NASA SSE (2012): Surface meteorology and Solar Energy. http://eosweb.larc.nasa.gov/sse/

Norris, B. L., Hoff, and T. E., (2011): "Determining Storage Reserves for Regulating Solar Variability." Electrical Energy Storage Applications and Technologies Biennial International Conference 2011.

Mills, A., Wiser, R. (2010): Implications of Wide-Area Geographic Diversity for Short-Term Variability of Solar Power. Lawrence Berkeley National Laboratory Technical Report LBNL-3884E

PEA – Puerto Rico Energy Authority, (2013)

Perez, M., and V. Fthenakis, (2012): Quantifying Long Time Scale Solar Resource Variability. Proc. World Renewable Energy Forum, Denver, CO.

Perez, M., and V. Fthenakis, (2015): On the Spatial Decorrelation of Stochastic Solar Resource Variability at Long Timescales. Solar Energy, Forthcoming.

Perez, M. J. R., (2015): Geographic Dispersion and Curtailment of VLS-PV Electricity. IEA PVPS Task 8 report, Ch.4 Future Technical Options for the Entire Energy System, Forthcoming.

Perez, R., P. Ineichen, R. Seals and A. Zelenka, (1990): Making Full Use of the Clearness Index for Parameterizing Hourly Insolation Conditions. Solar Energy 45, pp. 111-114

Perez, R., T. Hoff and S. Kivalov, (2011a): Spatial & temporal characteristics of solar radiation variability. Proc. of International Solar Energy (ISES) World Congress, Kassel, Germany

Perez, R., Kivalov, S., Schlemmer, J., Hemker Jr., C., Hoff, T. E. (2011b): Parameterization of site-specific short-term irradiance variability, Solar Energy 85 (2011) 1343-1353.

Perez, R., Kivalov, S., Schlemmer, J., Hemker Jr., C., Hoff, T. E. (2012): "Short-term irradiance variability correlation as a function of distance." Accepted to Solar Energy (Feb. 2012).

Perez, R., and T. Hoff, (2013): Solar Resource Variability, in: Solar Resource Assessment and Forecasting (Editor Jan Kleissl), Elsevier, 2013

Perez, R., T. Hoff, J. Dise, D. Chalmers and S. Kivalov (2013b): Mitigating Short-Term PV Output Variability Proc. 28th European Photovoltaic Solar Energy Conference and Exhibition (EUPVSEC), Paris, France.

Perez, R., A. Kankiewicz, J. Schlemmer, K. Hemker , Jr., and S. Kivalov, (2014): A New Operational Solar Resource Forecast Service for PV Fleet Simulation, in 40th IEEE PV Specialists Conference, 2014

Rowlands, I.H., Kemery, B.P., and Beausoleil-Morrison, I. (2014): Managing Solar-PV Variability with Geographical Dispersion: An Ontario (Canada) Case-Study. Renewable Energy 68:171-180

Sengupta, (2011): Measurement and Modeling of Solar and PV Output Variability. Proc. Solar 2011, American Solar Energy Society Conf., Raleigh, NC

Skartveit A., and J. A. Olseth, (1992): The Probability Density of Autocorrelation of Short-term Global and beam irradiance. Solar Energy, Volume 46, No. 9, pp. 477-488.

Stein, J., A. Ellis, C. Hansen, V. Chadliev, (2011): Simulation of 1-Minute Power Output from Utility-Scale Photovoltaic generation Systems. Proc. Solar 2011, American Solar Energy Society Conf., Raleigh, NC

Stokes, G.M., and S. E. Schwartz, (1994): The atmospheric radiation measurement (ARM) program: programmatic background and design of the cloud and radiation test bed. Bulletin of American Meteorological Society 75, 1201–1221

Urquhart, B., Kurtz, B., Dahlin, E., Ghonima, M., Shields, J. E., and J Kleissl.: Development of a sky imaging system for short-term solar power forecasting, Atmos. Meas. Tech. Discuss., 7, 4859-4907, doi:10.5194/amtd-7-4859-2014, 2014.

Vignola, F., (2001): Variability of Solar Radiation over Short Time Intervals, Proc. Solar 2001, American Solar Energy Society Conf., Washington, D.C

Vindel, J.M. and J. Polo, (2014). Intermittency and Variability of Daily Solar Irradiation. Atmospheric Research 143:313-327

Wiemken E., H. G. Beyer, W. Heydenreich and K. Kiefer (2001): Power Characteristics of PV ensembles: Experience from the combined power productivity of 100 grid-connected systems distributed over Germany. Solar Energy 70, 513-519

Woyte, A., Belmans, R., Nijs, J. (2007): “Fluctuations in instantaneous clearness index: Analysis and statistics.” Solar Energy 81 (2), 195-206.

Yang, H, B Kurtz, A Nguyen, B Urquhart, CW Chow, M Ghonima, J **Kleissl**, Solar irradiance forecasting using a ground-based sky imager developed at UC San Diego, Solar Energy, 103: 502-524, 2014.

Yordanov, G., O. Mitdgard, O. and L. Norum (2013): Overirradiance (Cloud Enhancement) Events at High Latitudes. IEEE Journal of Photovoltaics, 3, 1, 271-278